PHYSICAL REVIEW B VOLUME 32, NUMBER 12 15 DECEMBER 1985

Theoretical study of electrical conduction in finite metals and insulators

G. Kirczenow
Department of Physics, Simon Fraser University, Burnaby, British Columbia, Canada V5A 1S6
(Received 18 June 1985)

A tight-binding model is presented which is suitable for numerical simulations of electrical conduction in finite multiband systems driven by a time-dependent vector potential. The systems studied are linear chains of static atoms with periodic boundary conditions. The time evolution of the electrons is followed by integrating numerically the equations of motion of the density matrix. Dimerized finite chains with one electron per atom, i.e., insulators, are found to exhibit undamped periodic current oscillations in a steady moderate electric field. These oscillations are interpreted in terms of the single-band acceleration theorem (SBAT) for finite insulators. At higher fields the SBAT breaks down and Zener tunneling is studied in different regimes. The effect of the presence of impurities on the electric currents in both insulating and metallic chains of atoms is also studied. The relationship between the present work and the London theory of ring currents in cyclic molecules in a magnetic field is discussed.

I. INTRODUCTION

At the present time, most theoretical work on electrical conduction in solids is based on the Kubo formula or the Boltzmann equation. These approaches have been very successful, so much so that they have come to define the standard conceptual framework for thinking about transport problems. However, they have certain limitations. The Boltzmann equation is inherently semiclassical. While the Kubo formula is exact, it is applicable only to linear response. Also, its applicability is limited mainly to the study of thermodynamic averages, namely, the transport coefficients. Thus, the possibility of obtaining exact and complete microscopic information about nonlinear current-carrying systems by solving numerically the quantum equations of motion of the electrons in the time domain is very appealing. However, little such work has been done. In this article the feasibility of such calculations is explored and a number of interesting results concerning electrical conduction in some simple finite systems are presented.

In order for such an approach to be successful, it is necessary to use a discretized theory and to work with a small number of electronic bands. Thus, it is crucial to choose a good restricted basis and an appropriate Hamiltonian. In Sec. II a tight-binding formulation of this kind is presented, which is particularly suitable for use with periodic boundary conditions. It is set up originally for the one-band case, and then multiband effects are studied by introducing a periodic lattice distortion which splits the original band.[1] Depending on the choice of the distortion and the filling of the available states by electrons, the case of a metal or of an insulator can be studied. Here the case of noninteracting electrons in a finite one-dimensional chain will be considered with periodic boundary conditions. The lattice distortion chosen for most of the calculations reported here has a period of two atomic spacings, so that the system has two bands. The electric field is introduced by means of a time-dependent vector potential. The electrons are taken to be in the ground state at $t=0$ when the electric field is switched on smoothly from zero. The subsequent time evolution of the system is studied by integrating numerically the equations of motion of the electron-density matrix.

In Sec. III the results are presented for the case of metals and insulators with and without "isoelectronic" impurities. It turns out that a finite insulator with periodic boundary conditions is very different from the familiar case of an infinite insulator. The finite insulator exhibits periodic, undamped current oscillations in a steady electric field which is not too strong. These oscillations are not due to Zener breakdown (which only occurs for very high fields and/or small band gaps). Rather, the oscillations are closely related to the oscillations of Bloch electrons which would occur in a perfect metal in a strong steady electric field. However, in marked contrast with the case of a metal, the oscillations in the finite insulator are extremely stable. They are not damped by scattering from impurities or lattice imperfections, although their amplitude is somewhat lower in the presence of strong scattering centers than in the perfect crystal. The amplitude and period of the oscillations decrease with increasing length of the chain so that the usual passive behavior of insulators is recovered in the long-chain limit. The finite perfect metal exhibits the expected current oscillations in a steady electric field, but when an imperfection is introduced into the chain, the simple oscillations are replaced by a complex high-frequency behavior whose amplitude fluctuates but does not decay with time.

Also in Sec. III, Zener breakdown is studied by beginning with the insulating case and examining the behavior as the electric field is increased, or the band gap is reduced by reducing the amplitude of the lattice distortion. Different regimes are studied, each with its own characteristic current pattern.

It should be noted that the electric currents studied in this article are all purely electronic in origin. They are *not* due to the sliding charge-density waves which are ob-

 ©1985 The American Physical Society

served in some quasi-one-dimensional conductors, since the sliding charge-density waves involve the vibrational motion of the atoms, and in the present model the atoms are assumed to be fixed. However, it is clear that a good understanding of the electronic currents in static finite chains needs to be obtained before one can use finite chains with periodic boundary conditions to model the microscopic physics of sliding charge-density wave conduction.

This work also offers a different and complementary perspective of the physics of finite crystals in an electric field to that which is presented by the theoretical investigations of Stark ladders in finite systems (see Ref. 2 for a recent study in this field and further references). The work on Stark ladders has been concerned mainly with the energy spectrum of electronic states in the presence of an electric field derived from a scalar potential, while this study examines the time-dependent currents in similar systems, but where the electric field is derived from a vector potential. The latter feature of the present work is appropriate for transport calculations if periodic boundary conditions are used. In Sec. IV the relationship between this work and the London theory of ring currents in aromatic molecules[3] is examined.

II. THE TIGHT-BINDING FORMALISM

It is well known that if periodic boundary conditions are to be used, them the most consistent way to formulate the problem of electrical conduction in a solid is to introduce the electric field by means of a time-dependent vector potential. Since the tight-binding approximation and its refinements are widely used in solid-state physics, a generalization of the tight-binding Hamiltonian which includes the effects of such a vector potential should be of general interest. Surprisingly, no such generalization appears to be widely known among solid-state physicists, although the London Hamiltonian describing the related problem of ring molecules in a steady magnetic field was put forth many years ago.[2] A simple formulation in a solid-state context will be given in this section.

A. Single-band Hamiltonian and current operator

In the absence of the electric field, the tight-binding electron Hamiltonian is

$$H_0=\sum_{i,j,s} t_{ijs}c_{is}^{\dagger}c_{js} \ , \tag{1}$$

where

$$t_{ijs}=\langle \phi_{is} \mid (p^2/2m+V) \mid \phi_{js} \rangle \ , \tag{2}$$

$c_{is}^{\dagger}$ creates an electron in a state $\mid \phi_{is} \rangle$ belonging to band s and located in the neighborhood of site i, and V is the periodic potential of the lattice. Unless otherwise stated, spin variables will be suppressed and summations over them understood. We include the effect of an electric field $\mathbf{E}$ by introducing a time-dependent vector potential $\mathbf{A}$, assumed for simplicity to be spatially uniform in the region of interest. Then

$$\mathbf{E}=\frac{-\partial \mathbf{A}}{\partial t} \tag{3}$$

and the Hamiltonian becomes

$$H_A=\sum_{i,j,s,s'} t_{isjs'}^{A}c_{is}^{\dagger}c_{js'} \ , \tag{4}$$

where

$$t_{isjs'}^{A}\equiv\langle \phi_{is} \mid [(\mathbf{p}-q_e\mathbf{A})^2/2m+V] \mid \phi_{js'} \rangle=\langle \phi_{is} \mid \exp(iq_e\mathbf{r}\cdot\mathbf{A}/\hbar)(p^2/2m+V)\exp(-iq_e\mathbf{r}\cdot\mathbf{A}/\hbar) \mid \phi_{js'} \rangle$$
$$=\sum_{k,l,s''} \langle \phi_{is} \mid \exp(iq_e\mathbf{r}\cdot\mathbf{A}/\hbar) \mid \phi_{ks''} \rangle t_{kls''} \langle \phi_{ls''} \mid \exp(-iq_e\mathbf{r}\cdot\mathbf{A}/\hbar) \mid \phi_{js'} \rangle \ , \tag{5}$$

and q_e is the charge of an electron.

The choice of the tight-binding states $\mid \phi_{is} \rangle$ is crucial. In general, if Wannier states are used, H_0 is band diagonal as in Eq. (1). Since $\mathbf{r}$ is a Hermitian operator, one can always choose the $\mid \phi_{is} \rangle$ to be linear combinations of Wannier states belonging to band s, such that

$$\langle \phi_{is} \mid \mathbf{r} \mid \phi_{js} \rangle=\mathbf{r}_{is}\delta_{ij} \ . \tag{6}$$

Thus, H_0 remains band diagonal and $\mathbf{r}$ is now site diagonal within any band, although, of course, $\mathbf{r}$ is not band diagonal. A representation having just these properties was recently used by Roy and Mahapatra[2] to study the energy spectrum of Stark ladders.

A "single-band" Hamiltonian describing a particular band s can now be obtained by omitting from the above expression for $t_{isjs'}^{A}$, all terms involving other bands, yielding

$$H=\sum_{i,j} t_{ijs}\exp[iq_e\mathbf{A}\cdot(\mathbf{r}_{is}-\mathbf{r}_{js})/\hbar]c_{is}^{\dagger}c_{js} \ . \tag{7}$$

In other words, in the single-band approximation, the vector potential simply phase shifts the hopping matrix elements t_{ijs} by an amount depending on the separation of the sites i,j. The electrical current-density operator is

$$\mathbf{j}_A=q_e[\mathbf{r},H_A]/\Omega i\hbar \ , \tag{8}$$

where Ω is the volume. Using the same basis states and again omitting interband matrix elements of $\mathbf{r}$ and H^A yields a single-band current-density operator for band s

$$\mathbf{j}=[q_e/(\Omega i\hbar)]\sum_{i,j} t_{ijs}(\mathbf{r}_{is}-\mathbf{r}_{js})\times\exp[iq_e\mathbf{A}\cdot(\mathbf{r}_{is}-\mathbf{r}_{js})/\hbar]c_{is}^{\dagger}c_{js} \ . \tag{9}$$

The physical content of Eqs. (7) and (9) can be understood very simply as follows. Suppose for $t\leq 0$, $\mathbf{E}=\mathbf{A}=\mathbf{0}$, and after $t=0$, the electric field is smoothly switched on by varying $\mathbf{A}$ appropriately. If $\mathbf{A}$ is spatially uniform and the $\{\mathbf{r}_{is}\}$ form a Bravais lattice, it follows

that the solutions Ψ of the one-band Schrödinger equation

$$i\hbar\frac{\partial\Psi}{\partial t}=H\Psi \tag{10}$$

for a single electron have the form

$$\Psi(t)=\frac{1}{\sqrt{N}}\gamma(t)\sum_i e^{i\mathbf{k}\cdot\mathbf{r}_i}\,|\,\phi_{is}\,\rangle\ , \tag{11}$$

where N is the number of Bravais lattice vectors and $\gamma(t)$ is a phase factor obeying

$$i\hbar\frac{\partial\gamma}{\partial t}=\epsilon_s(\mathbf{k}-q_e\mathbf{A}/\hbar)\gamma\ , \tag{12}$$

where

$$\epsilon_s(\mathbf{k})=\sum_j t_{ijs}e^{i\mathbf{k}\cdot(\mathbf{r}_j-\mathbf{r}_i)}\ . \tag{13}$$

$\epsilon_s(\mathbf{k})$ is the energy of Bloch state $|\,\mathbf{k},s\,\rangle$ in the absence of external fields. The wave vector $\mathbf{k}$ of the state is a good quantum number as expected for the uniform vector potential $\mathbf{A}$. Using (9) and (13), the current density in state Ψ is

$$\langle\Psi\,|\,\mathbf{j}\,|\,\Psi\rangle=\frac{q_e}{\Omega}\frac{1}{\hbar}\left[\frac{\partial\epsilon_s}{\partial\mathbf{q}}\right]_{\mathbf{q}=\mathbf{k}-q_e\mathbf{A}/\hbar}, \tag{14}$$

i.e.,

$$\langle\Psi\,|\,\mathbf{j}\,|\,\Psi\rangle=\frac{q_e}{\Omega}\frac{1}{\hbar}\left[\frac{\partial\epsilon_s}{\partial\mathbf{q}}\right]_{\mathbf{q}=\mathbf{k}+\hbar^{-1}q_e\int_0^t\mathbf{E}(t')dt'}. \tag{15}$$

This is the current which is predicted by the familiar acceleration theorem

$$\frac{d\mathbf{k}}{dt}=\frac{q_e\mathbf{E}}{\hbar} \tag{16}$$

for an electron which begins in a Bloch state with wave vector $\mathbf{k}$ at time $t=0$, and is subsequently accelerated by an electric field $\mathbf{E}$. The validity of using (16) in a single-band approximation has in the past been questioned.[4] However, at present it is widely believed to be correct for large band gaps and/or small fields.[2,5,6] The numerical calculations for the two-band systems which are described in Sec. III lend additional support to the validity of the single-band equation (15) under these conditions. The above results suggest that the Hamiltonian (7) and the current operator (9) contain the essential physics of Bloch equation propagation in a single-band approximation in a perfect crystal. For finite crystals, states with only discrete values of $\mathbf{k}$ are allowed. Nevertheless, the function $\epsilon_s(\mathbf{k})$ is defined for *all* values of $\mathbf{k}$ by expression (13), and the variable $\mathbf{q}$ in (15) sweeps a continuum of values, resulting in a smoothly varying current. Henceforth, we shall consider only the particular band s and suppress the subscript s from all symbols.

B. Splitting the band

In the above treatment the lattice sites (or in simple cases, atoms) are evenly spaced. We would like, however, to also consider distortions from this periodicity within the same tight-binding scheme. We can do this by identifying the $\{\mathbf{r}_i\}$ with the positions of the atoms and the t_{ij} with the resonance integrals involving the tight-binding states on atoms i and j. Adopting such a simple tight-binding view and restricting ourselves to nearest-neighbor hopping, it seems reasonable to apply the results (7) and (9) directly to the case of unequally spaced atomic sites $\mathbf{r}_i$, assuming that the resonance integrals t_{ij} are a smooth function of the displacement $\mathbf{r}_i-\mathbf{r}_j$ between sites i and j.

Although this approach in the spirit of the tight-binding method is physically appealing, it is difficult to justify in detail. It has been successfully used to describe the electronic structure of polyacetylene[7] but in the absence of electric currents. Further justification of the application of this approach to the present problem will be provided by the numerical results presented in Sec. III and by the comparison made in Sec. IV with the work on ring currents in aromatic molecules in magnetic fields.

We will consider periodic distortions which have the effect of splitting the tight-binding band. Such distortions are common in quasi-one- and two-dimensional materials where they often occur spontaneously because of the Peierls mechanism.[8] Perhaps the simplest system of this kind is polyacetylene $(CH)_x$ and we will use it as the prototype for the structures to be considered in this paper. Polyacetylene is based on a chain of carbon atoms linked by alternating slightly longer and shorter bonds. This "dimerization" splits in half the highest electronic band which is half filled with π electrons, resulting in a gap at the Fermi energy. Of course, the dimerization is itself driven by the reduction in electronic energy which accompanies the opening of this gap.

As a further simplification we will consider only completely linear structures with the axis and all bonds aligned parallel to the direction of A. The Hamiltonian (7) for nearest-neighbor hopping then becomes

$$H=\sum_n\left(t_{n+1,n}\exp[iq_eA(a+u_{n+1}-u_n)/\hbar]c_{n+1}^\dagger c_n\right.$$
$$\left.+t_{n,n+1}\exp[-iq_eA(a+u_{n+1}-u_n)/\hbar]c_n^\dagger c_{n+1}\right)\ , \tag{17}$$

where $t_{n,n}=0$ has been chosen, a is the average atomic spacing along the chain, and u_n is the displacement from the undistorted position at the nth site. Following Ref. 7, we will take $t_{n+1,n}$ to be real and expand it to leading order in the displacements. Then,

$$t_{n+1,n}=t_{n,n+1}\cong-[t_n+\alpha(u_{n+1}-u_n)]\ , \tag{18}$$

where the minus sign is inserted for convenience. Likewise, the electric current operator becomes

$$j=\frac{q_e}{i\hbar L}\sum_n\left(t_{n+1,n}(a+u_{n+1}-u_n)\exp[iq_eA(a+u_{n+1}-u_n)]c_{n+1}^\dagger c_n\right.$$
$$\left.-t_{n,n+1}(a_n+u_{n+1}-u_n)\exp[-iq_eA(a+u_{n+1}-u_n)]c_n^\dagger c_{n+1}\right)\ , \tag{19}$$

where L is the length of the chain.

In a perfectly dimerized chain, the displacements u_n take the form

$$u_n=(-1)^n u \ . \tag{20}$$

In polyacetylene in the absence of external fields, the amplitude u is determined by a competition between the energy of the π electrons described by the Hamiltonian H (which favors dimerization) and the σ-bond energy which favors a uniform chain. In Ref. 7 the latter contribution is modeled by a harmonic term

$$E_\sigma=\tfrac{1}{2}\sum_n K(u_{n+1}-u_n)^2 \ ,$$

and u is found by minimizing the total energy. In this paper the u_n will not be obtained in that way. Instead, u will be regarded simply as a parameter whose value will be chosen at will and which will be used to set the magnitude of the splitting of the tight-binding band of our model system to any desired value.

The band structure described by the Hamiltonian (17) for the distortion $\{u_n\}$ given by (20) in the absence of the vector potential A, and assuming periodic boundary conditions, is as follows: The Brillouin zone for the two-atom unit cell extends from $-\pi/2a$ to $\pi/2a$ and there are two bands, an upper band labeled $+$ and a lower band labeled $-$. The eigenstates are Bloch states which can be written in the form

$$\Psi_k^{\pm}=\frac{1}{\sqrt{N}}\sum_n e^{ikan}b_n^{\pm}(k)\,|\,\phi_n\rangle \ , \tag{21}$$

where for each k allowed by periodic boundary conditions, $b_n^{\pm}(k)$ takes two values

$$b_n^{\pm}(k)=\begin{cases} b_e^{\pm}(k) & \text{if } n \text{ is even,} \\ b_0^{\pm}(k) & \text{if } n \text{ is odd,} \end{cases} \tag{22}$$

the coefficients $b_e^{\pm}(k)$ and $b_0^{\pm}(k)$ satisfy the secular equations

$$\begin{aligned} &[(1-\beta)e^{ika}+(1+\beta)e^{-ika}]b_e+\xi_k b_0=0 \ , \\ &\xi_k b_e+[(1+\beta)e^{ika}+(1-\beta)e^{-ika}]b_0=0 \ , \end{aligned} \tag{23}$$

where

$$\beta=-2\alpha u/t_0 \ , \tag{24}$$

and the energy eigenvalues $\epsilon^{\pm}(k)$ corresponding to the states $\Psi_k^{\pm}$ [Eq. (21)] are given by

$$\epsilon^{\pm}(k)=t_0\xi_k \ . \tag{25}$$

Explicitly,

$$\epsilon^{\pm}(k)=\pm\{[2t_0\cos(ka)]^2+[4\alpha u\sin(ka)]^2\}^{1/2} \ . \tag{26}$$

The band gap which occurs because of the lattice distortion at $k=\pm\pi/2a$ has a magnitude

$$\Delta=8\alpha u \ , \tag{27}$$

which is proportional to the amplitude of lattice distortion. When the electric field is switched on, the Hamiltonian (17) mixes the states $\Psi_k^{\pm}$ of the two bands but does not mix states with different k values.

it should be noted that very recently Roy and Mahapatra[2] used a two-band tight-binding approximation in their study of Stark ladders in an electric field. Their approach was to take two tight-binding bands (which are completely noninteracting in the absence of the electric field), each with a sinusoidal $\epsilon(k)$, and to include the electric-field-induced interband matrix elements using expressions based on $\mathbf{k}\cdot\mathbf{p}$ theory. The present Hamiltonian is somewhat different and would seem to be appropriate for small and moderate band gaps, and should thus be capable of handling Zener tunneling. The fact that the two split bands in the present formalism are not sinusoidal [as is clear from Eq. (26) for $\epsilon\pm(k)$] turns out to have very important consequences for the problem of electrical conduction in finite systems, as will be demonstrated below. A Stark ladder analysis of the present system and a careful comparison with the results, which were obtained by Roy and Mahapatra[2] using the $\mathbf{k}\cdot\mathbf{p}$ approach, would be of considerable interest, but will not be pursued here.

III. CALCULATIONS AND RESULTS

A. Equations of motion and boundary conditions

In this section the time evolution of systems containing several electrons will be studied by solving numerically the equations of motion of the electron-density matrix. Single-particle density matrices are appropriate since electron-electron interactions are not included in the calculations. The representation used is that of the tight-binding states $|\,\phi_n\rangle$. This choice is convenient because only nearest-neighbor hopping is contained in the Hamiltonian, resulting in relatively simple equations of motion for the density matrix, even when impurity scattering of the electrons is included in the calculation.

The density-matrix equation of motion is

$$i\hbar\dot{\rho}=[H,\rho] \ . \tag{28}$$

With the notation

$$\rho_{kl}=\langle\phi_k\,|\,\rho\,|\,\phi_l\rangle \ , \tag{29}$$

(28) yields

$$\begin{aligned} \dot{\rho}_{kl}=i\{&[t_0+\alpha(u_k-u_{k-1})]\exp[iq_eA(a+u_k-u_{k-1})/\hbar]\rho_{k-1,l} \\ &+[t_0+\alpha(u_{k+1}-u_k)]\exp[-iq_eA(a+u_{k+1}-u_k)/\hbar]\rho_{k+1,l} \\ &-[t_0+\alpha(u_{l+1}-u_l)]\exp[iq_eA(a+u_{l+1}-u_l)/\hbar]\rho_{k,l+1} \\ &-[t_0+\alpha(u_l-u_{l-1})]\exp[-iq_eA(a+u_l-u_{l+1})/\hbar]\rho_{k,l-1}-(v_k-v_l)\rho_{kl}\} \ . \end{aligned} \tag{30}$$

In deriving (30) it was assumed that in addition to the periodic (or nonperiodic) distortion $\{u_n\}$ described by the Hamiltonian (17), impurity terms of the form $v_n c_n^\dagger c_n$ have been included in the Hamiltonian H.

The density matrices in this article will always be spin diagonal. This can be assumed because the Hamiltonians which are being considered are spin diagonal and we will only consider states in which there are always as many spin-up as spin-down electrons. Thus, the spin variables have only a trivial role and are not written explicitly in the above equations.

In the following calculations, $\rho(0)$, the density matrix at time $t=0$, is taken to be that of the system in its ground state. It is calculated by finding the eigenvalues and eigenstates of the Hamiltonian for $A=0$. If the eigenstates are of the form

$$\Psi_\mu = \sum_n g_{\mu n} | \phi_n \rangle , \tag{31}$$

then

$$\rho_{nm}^{(0)} = \sum_\mu{}' g_{\mu m} g_{\mu n}^* , \tag{32}$$

where the sum extends over the one-electron eigenstates which are *occupied* in the many-electron ground state. In the cases where the lattice distortion is perfectly periodic [Eq. (20)] and there are no impurities, it is straightforward to find $\rho_{nm}(0)$ analytically from Eqs. (21)—(26). However, in general, the initial density matrix was calculated from the eigenvectors and eigenvalues of the Hamiltonian which were found numerically.

Periodic boundary conditions are implemented for a chain of N atoms by defining

$$\begin{aligned} &\rho_{N+1,n} \equiv \rho_{1,n}, \quad \rho_{n,N+1} \equiv \rho_{n,1}, \quad \rho_{0,n} \equiv \rho_{N,n} , \\ &\rho_{n,0} \equiv \rho_{n,N}, \quad u_{N+1} \equiv u_1, \quad u_0 \equiv u_N , \end{aligned} \tag{33}$$

wherever the quantities on the left-hand side of (33) appear in the equations (30) or elsewhere in the calculations. Similarly, we identify $|\phi_{N+1}\rangle \equiv |\phi_1\rangle$, $|\phi_0\rangle \equiv |\phi_N\rangle$, $g_{\mu N+1} \equiv g_{\mu 1}$, and $g_{\mu 0} \equiv g_{\mu N}$ in defining the electronic states involved.

Starting at $t=0$, the electric field was switched on smoothly by varying the vector potential appropriately. In the results to be presented, the actual choice of the time dependence was

$$A = -\tilde{E} t^3/(t^2+t_r^2) . \tag{34}$$

The electric field $E=-\partial A/\partial t$ increases initially smoothly from 0 ($E \propto t^2$ for small t) and approaches a steady value $\tilde{E}$ for large times. t_r is a measure of the time which it takes to switch the electric field on. The rational polynomial form (34) switches the electric field on smoothly, but it should be noted that the approach to the steady state value $\tilde{E}$ is not monotonic, and the electric field actually has a maximum value of $\frac{9}{8}\tilde{E}$ which occurs at $t=\sqrt{3}t_r$.

The density matrix for times $t>0$ was calculated by integrating (30) numerically using a Runge-Kutta algorithm. The electric current at time t was found using

$$\langle j \rangle_t = \mathrm{Tr}(\rho j) . \tag{35}$$

The form (19) for the current operator was used whether impurity scattering was included in the Hamiltonian or not. This is justified because in the split-band tight-binding model described in Sec. II B, both the position operator r and the scattering potential $v_n c_n^\dagger c_n$ are considered to be diagonal in the representation $\{|\phi_n\rangle\}$, so that v_n does not contribute to the commutator defining the current operator.

B. Finite insulators

If we take a perfectly dimerized chain $[u_n=(-1)^n u]$ with one electron per atom, then in the ground state, the lower $(-)$ split band is completely filled with electrons and the upper $(+)$ band is empty. This is normally considered to be an insulator. We are not concerned with soliton-type structures[7] in this paper so that we will study only cases where N, the number of atoms in the chain, is even. The two cases $N=4n$ and $N=4n+2$, with n an integer, are somewhat different from each other.

We will consider the former case first, for $N=32$. The band structure and occupied levels in the ground state in the absence of fields for this case are shown in Fig. 1, for $t_0=2.5$ eV, $\alpha=4.1$ eV/Å, $u=0.0404$ Å. (These parameters have been used for polyacetylene in Ref. 7.) The closed circles are the occupied one-electron states; the open circles are the vacant one-electron states. The band gap Δ at the Brillouin-zone boundary is 1.325 eV. The response of this system to an electric field $\tilde{E}=10^7$ V/m switched on according to Eq. (34) with a rise time $t_r=10^{-13}$ s is summarized in Fig. 2. The average atomic spacing a was taken to be 1.22 Å. The behavior of the electric current is shown by the solid curves in Figs. 2(a)

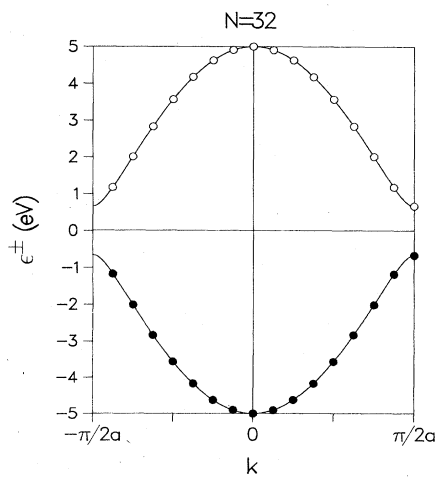

FIG. 1. Energy bands $\epsilon^{\pm}(k)$ of a perfectly dimerized 32-atom chain with one electron per atom. $t_0=2.5$ eV, $\alpha=4.1$ eV/Å, $u=0.0404$ Å. Closed circles represent the filled electron states, each containing two electrons, in the ground state of this system. Open circles represent empty one-electron states. The band gap Δ at $k=\pm\pi/2a$ is 1.325 eV.

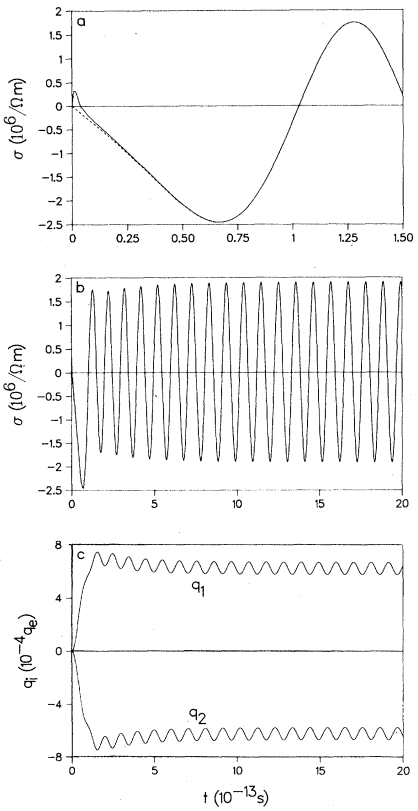

FIG. 2. (a) Time-dependent conductivity σ versus time for a 32-atom perfectly dimerized chain with one electron per atom in an electric field $\tilde{E}=10^7$ V/m switched on with a rise time t_r of 10^{-13} s. The electronic structure of the system in its ground state is that shown in Fig. 1. The solid line is the result of the numerical integration of the density-matrix equations of motion. The dashed line is the prediction of the single-band acceleration theorem for electrons in the lower split band. $a=1.22$ Å. (b) As for Fig. 2(a) but showing the behavior over a longer time interval. The dashed line and the solid line are indistinguishable on this scale except at very short times. (c) The net charge on atoms 1 and 2 as a function of time for the same system as in Figs. 2(a) and 2(b).

and 2(b). The quantity $\sigma(t)$, which is plotted, is a time-dependent "conductivity" defined by

$$\sigma(t)\equiv\frac{\langle j\rangle_t}{E(t)X} . \tag{36}$$

The quantity X in the denominator is a scale factor chosen to have units of area and a magnitude of 10 Å^2. If X is interpreted as the cross-sectional area of the atomic chain, then some feeling for the magnitude of the currents flowing in the chain can be obtained by comparing $\sigma(t)$ with the conductivities of bulk materials. Initially, the current begins to flow in the direction of the electric field, but then peaks and reverses direction at $t\simeq 4\times 10^{-15}$ s [Fig. 2(a)] and then begins to oscillate, the oscillations becoming very regular as the electric field approaches its asymptotic value $\tilde{E}$ [Fig. 2(b)]. By the above criterion, the amplitude of the oscillating current is quite large. Also, the oscillations show no indication of damping with time. The time dependence of the net charge q_i on atom i is shown in Fig. 2(c) for $i=1,2$. q_i is defined by

$$q_i=\sum_{\eta}(\rho_{i\eta,i\eta}-1)q_e , \tag{37}$$

where η stands for spin. As the field is switched on, the chain becomes polarized, alternate atoms becoming positively and negatively charged. The magnitude of the net charge $|q_i|$ is the same for all atoms i. The polarization charge oscillates with time as can be seen from Fig. 2(c). The period of the charge oscillations is the same as that of the current oscillations, but there is a $\pi/2$ phase shift relative to the current.

The presence of such undamped current oscillations in a system with a completely filled band is, at first sight, surprising. However, this behavior can be understood in a simple way as will be explained below.

Let us calculate the current which would be predicted for this system on the basis of the single-band acceleration theorem as applied only to the lower (—) split band which contains all of the electrons at $t=0$. In this single-band (SB) model the current is given by

$$\langle j_{\rm SB}(t)\rangle=\sum_{k,\eta}\frac{q_e}{L}\frac{1}{\hbar}\left[\frac{\partial\epsilon^-(q)}{\partial q}\right]_{q=k+\hbar^{-1}q_e\int_0^t E(t')dt'} , \tag{38}$$

where the sum is over the occupied one-electron electron states with wave vectors k (as represented in Fig. 1) and spins η. (Eq. 38) is a direct application of Eq. (15) to the lower split band. The conductivity

$$\sigma_{\rm SB}=\langle j_{\rm SB}(t)\rangle/E(t)X ,$$

which corresponds to this current, is represented by the dashed curve in Fig. 2(a). At very short times ($t\lesssim 2\times 10^{-14}$ s), there is a significant discrepancy between $\sigma_{\rm SB}$ and σ, the conductivity which was obtained by the numerical integration of the equations of motion of the density matrix. However, for longer times this discrepancy becomes progressively smaller, typically $\lesssim 0.1\%$ for $t\gtrsim 10^{-12}$ s.

The meaning of these results is as follows. The equation of motion of the density matrix which is solved numerically contains the physics of both the upper and lower split bands and of the transitions between the two bands which can be induced by an electric field. Although the electric field is switched on reasonably smoothly, there is nevertheless a transient response at very short times associated with the switching on process, and virtual transitions to the upper band dominate the very early behavior of the system. This results in the initial small peak which occurs in $\sigma(t)$ at $t\sim 10^{-15}$ s. Since these interband transitions do not conserve energy, their influence on the current soon becomes relatively very small, and then intraband processes which are confined to the lower split band dominate the electrical conduction process; hence, the excellent agreement between the predictions of the single-band acceleration theorem (38) and the results of the full numerical calculation which is found at later times.

The current oscillations which are shown in Fig. 2(b) occur because of the finite size of the system, which results in the finite separation in k space between the one-electron states in Fig. 1. The sum over k in expression (38) for the single-band current vanishes at $t=0$ because of the symmetry

$$\left[\frac{\partial\epsilon^{-}(q)}{\partial q}\right]_{q=k}=-\left[\frac{\partial\epsilon^{-}(q)}{\partial q}\right]_{q=-k}, \tag{39}$$

and because

$$\left[\frac{\partial\epsilon^{-}(q)}{\partial q}\right]_{q=0}=\left[\frac{\partial\epsilon^{-}(q)}{\partial q}\right]_{q=\pi/2a}=0 . \tag{40}$$

However, for general values of t there is no such cancellation, with the exception of times t such that

$$\hbar^{-1}q_e\int_0^t E(t')dt'=m\frac{\pi}{Na} , \tag{41}$$

where m is an integer and N is the number of atoms in the chain. Thus, the period T of the oscillations is the time which it takes for the wave vector q in expression (38) to travel between the wave vectors of two adjacent one-electron eigenstates shown in Fig. 1. In the limit when $E\rightarrow\tilde{E}$, we have

$$T=\frac{h}{|q_e|\tilde{E}Na} . \tag{42}$$

Thus, the period of the oscillations is inversely proportional to the chain length and to the electric field. The amplitude of the oscillations also decreases with increasing chain length, and in the limit of an infinite chain, when the one-electron states form a continuum in k space, (38) yields zero for the single-band current as expected.

It is clear that the oscillations which have been described above for a finite insulator are closely related to the Zener oscillations which are predicted for a perfect metal in a strong electric field. They should be a common feature of finite insulators with a wide variety of band structures. It is easy to show, however, that if the filled band under consideration has an energy dispersion which is exactly sinusoidal in $\mathbf{k}$ space, then $\langle j_{SB}(t)\rangle=0$ for all t. For this reason the two-band tight-binding model used by Roy and Mahapatra[2] in their recent study of Stark ladders will not exhibit such current oscillations if the lower band is completely filled with electrons. The excellent agreement between the predictions of the single-band acceleration theorem and the numerical calculations of the electric current in the two-band system for long times provides strong support for the validity of the single-band acceleration theorem under the present conditions.

The calculations described above for the $N=32$ system were repeated for chains of 16, 8, and 4 atoms using the same parameters as for the 32-atom chain. The results were qualitatively quite similar to those obtained for the 32-atom chain. For sufficiently long times t after the field was switched on, excellent agreement was obtained between the numerical calculations and the predictions of the single-band acceleration theorem. The period of the current oscillations was inversely proportional to the chain length as expected, and the amplitude of the oscillations increased with decreasing chain length.

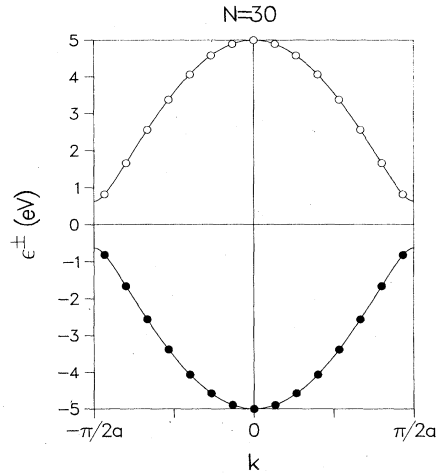

FIG. 3. Energy bands of a perfectly dimerized 30-atom chain in its ground state. $t_0=2.5$ eV, $\alpha=4.1$ eV, $u=0.0385$ Å. Notation as in Fig. 1.

The case $N=4n+2$ is somewhat different from that of $N=4n$ because of the different arrangement of the one-electron states near the top of the lower split band. This is illustrated in Fig. 3 for the case $N=30$. The essential qualitative difference between this case and that of $N=32$ (Fig. 1) is that here the highest occupied one-electron state is located not at the top of the lower split band (as in Fig. 1) but somewhat below it. The response of this system to the same electric field as that which was applied to the 32-atom chain above is shown in Fig. 4. $\sigma(t)$ again exhibits a small transient peak for $t\sim10^{-15}$ s. Excellent agree-

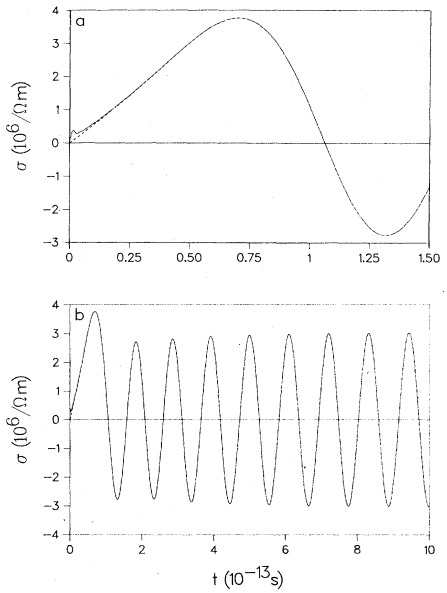

FIG. 4. Time-dependent conductivity for a perfectly dimerized 30-atom chain. $\tilde{E}=10^7$ V/m, $t_r=10^{-13}$ s. Structural and electronic parameters as in Fig. 3. Notation as in Fig. 2. $a=1.22$ Å.

ment is again found with the predictions of the single-band acceleration theorem at later times. An interesting feature is that the initial phase of the current oscillations is shifted by π from that in the 32-atom case. This initial phase difference is always found between the current oscillations in the dimerized chains of length $4N$ and $4N+2$, and it will be discussed further in Sec. IV.

Results consistent with the above were found also for weaker electric fields $\tilde{E}$. However, while the period of the current oscillations increases as the electric field decreases, the smallest time step which could be used in the numerical integration of the density-matrix equations of motion was found to be less sensitive to the size of $\tilde{E}$ for small fields. This limited the calculations which were carried out for weak fields to times which were relatively short on the scale of the period of the current oscillations.

C. Zener breakdown

If the value of the electric field $\tilde{E}$ is increased substantially beyond the values discussed in Sec. III B while keeping the other system parameters unchanged, the agreement between the predictions of the single-band acceleration theorem and the numerical calculations begins to deteriorate. In Fig. 5 the results are shown for the same 32-atom chain which was considered above (Figs. 1 and 2) but with a value of the electric field ten times larger, $\tilde{E}=10^8$ V/m. It is apparent that the very short-time transient response associated with the switching on of the field has become considerably stronger relative to the long-time oscillatory response. Also, the discrepancy between the single-band acceleration theorem and the calculated current at long times is much larger ($\sim 10\%$). However, the current oscillations are quite stable and no tendency for the magnitude of the discrepancy to change with time was found at later times, although times up to 10^{-12} s were studied. Thus, under these conditions, although the presence of the upper split band does have a significant influence on the response of the system, Zener breakdown does not appear to be taking place.

Increasing the field still further to $\tilde{E}=10^9$ V/m in the same system brings marked qualitative changes in the behavior. The early stages of the time evolution for the same 32-atom chain as above for $\tilde{E}=10^9$ V/m with a rise time $t_r=10^{-13}$ s are shown in Fig. 6. Initially, there is the usual transient response associated with the switching on of the electric field. Then, while the field is still relatively weak, the single-band-model current (dashed curve) follows the numerically calculated current (solid curve) fairly closely for a few cycles, although the agreement is not as good as for the weaker-field case shown in Fig. 5. As the electric field grows further, the amplitude of the current oscillations grows dramatically, and for $t \gtrsim 4\times 10^{-14}$ s the single-band model fails to provide even a qualitative description of the system. The amplitude of the calculated current oscillations becomes much larger than in the single-band model, and the current oscillations become rather irregular with pronounced higher-frequency compounds. The calculated current at later times is shown in Fig. 7. For $t \gtrsim 1.5\times 10^{-13}$ s, a new pattern emerges. There are current oscillations with both high- and low-frequency components. Particularly strik-

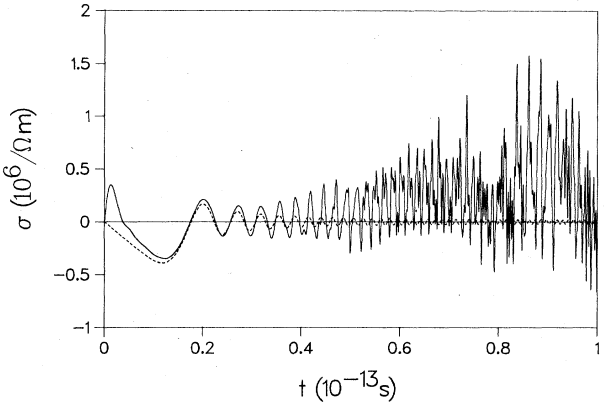

FIG. 6. Time-dependent conductivity for a perfectly dimerized 32-atom chain. Notation and parameters are the same as in Figs. 1 and 2, except that $\tilde{E}=10^9$ V/m. The onset of Zener breakdown is seen as the strength of the electric field increases with time.

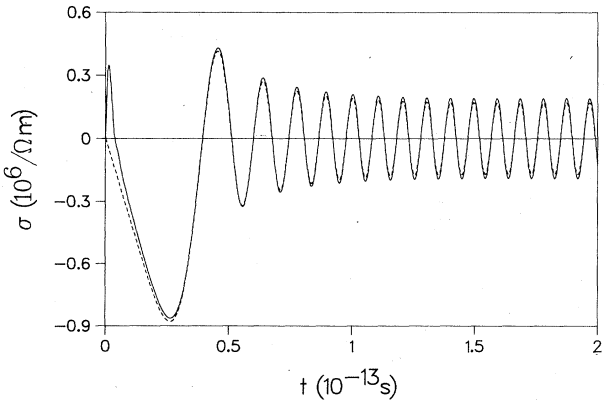

FIG. 5. Time-dependent conductivity for a perfectly dimerized 32-atom chain. Notation and parameters are the same as in Figs. 1 and 2, except that $\tilde{E}=10^8$ V/m.

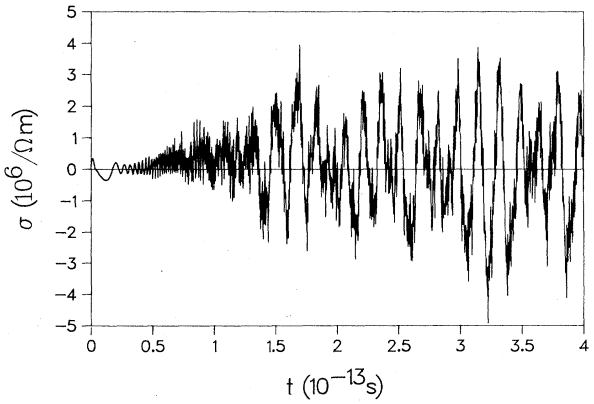

FIG. 7. Time-dependent conductivity for the same case in Fig. 6, but followed over a longer period of time. The current predicted by the single-band model is not shown.

ing is the strong, although somewhat unstable, component oscillation with a period $\tau \sim 1.7\times10^{-14}$ s. This should be compared with the Zener period (the time which it takes a Bloch electron to traverse the Brillouin zone), which for this dimerized chain for the limiting electric field $\tilde{E}$, is given by

$$T_z = \frac{h}{2a\,|\,q_e\,|\,\tilde{E}} \,. \tag{43}$$

For the present system with $a = 1.22$ Å, $\tilde{E} = 10^9$ V/m, (43), yields $T_z = 1.70\times10^{-14}$ s. Because the current oscillations greatly exceed the predictions of the single-band model in amplitude and because of the good agreement between τ and T_z, it is reasonable to suppose that Zener breakdown is taking place, that transitions between the upper and lower bands are occurring, and that the calculated current is due primarily to electrons which are being excited into the upper band and the holes which are left in the lower band.

It is interesting to compare these results with the simple standard expression for the probability of tunneling across the band gap by an electron in a strong electric field, as it passes the Brillouin zone boundary where the gap between the upper and lower bands is smallest.[9] For the present band structure, this probability is given approximately by

$$P \simeq \exp\left[-\frac{\pi^2}{16}\,\frac{\Delta^2}{t_0\,|\,q_e\,|\,Ea}\right] . \tag{44}$$

Setting $E = \tilde{E}$, this yields $P \simeq 4\times10^{-16}$ for the case $\tilde{E} = 10^8$ V/m considered above, which is consistent with our interpretation that Zener breakdown is not occurring in Fig. 5. However, for the case $\tilde{E} = 10^9$ V/m (Figs. 6 and 7), $P \simeq 3\times10^{-2}$. Such a tunneling probability would imply that the transfer of an electron between the two split bands occurs on the average on a time scale of several Zener periods T_z, (43). This is qualitatively consistent with the occurrence of somewhat irregular large-amplitude current oscillations with a period close to the Zener period, such as those which are seen in Fig. 7.

A case in which the Zener tunneling is even more favored is shown in Figs. 8 and 9, where the system is a 14-atom perfectly dimerized chain, but the distortion amplitude $u = 0.001$ Å is substantially smaller than in the cases considered above. The other band parameters $t_0 = 2.5$ eV, $\alpha = 4.1$ eV/Å, $a = 1.22$ Å are, as above, yielding a small band gap $\Delta = 3.28\times10^{-2}$ eV at the Brillouin-zone boundary. Note, however, that since $N = 14$ belongs to the class $N = 4n + 2$, the electronic structure is qualitatively similar to that of the $N = 30$ chain shown in Fig. 3, in that there is no one-electron state with a wave vector exactly at the zone boundary where the band gap is smallest. The electric field is switched on with a rise time $t_r = 10^{-13}$ s to a limiting value of $\tilde{E} = 3\times10^7$ V/m. For this limiting electric field, the Zener tunneling probability given by the simple expression (44) is $P \simeq 0.93$.

The early behavior of this system is shown in Fig. 8. The solid curve is the calculated response. The dashed curve is the prediction of the single-band acceleration theorem for the lower band. The dashed-dotted curve is the prediction of the single-band acceleration theorem for the case $u = 0$, where there is no distortion of the chain at all and only a single band is present. This corresponds to a perfect metal with no gap at the Fermi level.

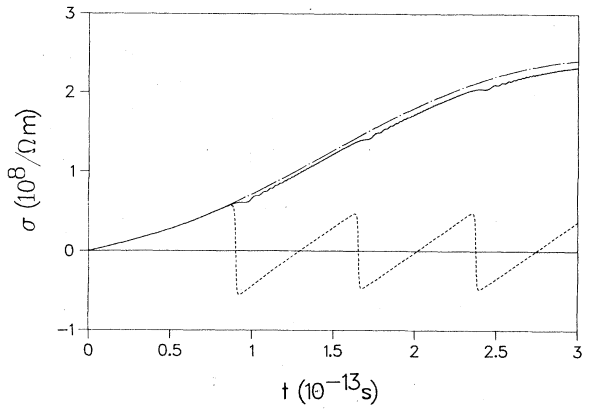

FIG. 8. Time-dependent conductivity for a 14-atom weakly dimerized chain with strong Zener tunneling. $u = 0.001$ Å, $t_0 = 2.5$ eV, $\alpha = 4.1$ eV/Å, $a = 1.22$ Å, $t_r = 10^{-13}$ s, $\tilde{E} = 3\times10^7$ V/m. The solid curve is the calculated result. The dashed curve is the prediction of the single-band acceleration theorem for the lower band only. The dashed-dotted curve is the prediction of the single-band acceleration theorem for $u = 0$.

The single-band acceleration theorem for the lower band does not allow for any Zener tunneling to the upper band. It predicts the simple saw-tooth current shown in Fig. 8 for the following reason. If tunneling to the upper band is not allowed, then, when the q vector [Eq. (15)] of any electron reaches the Brillouin-zone boundary it is Bragg reflected and the sign of the current carried by that electron changes. For such a small lattice distortion, $\epsilon^-(q)$ differs appreciably from $\epsilon(q)$ (the electron energy for the undistorted chain) only in a very narrow range near the zone boundary. This means that the current predicted by the single-band acceleration theorem for the lower band reverses almost discontinuously when the Bragg reflection occurs, resulting in the saw-tooth form.

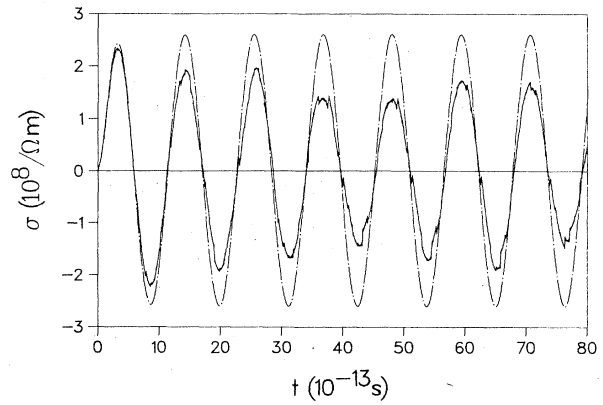

FIG. 9. Time-dependent conductivity for the same system as in Fig. 8 but extending over a longer period of time. The prediction of the single-band acceleration theorem for the lower band is not shown.

Until the q vector of the first electron reaches the immediate vicinity of the Brillouin-zone boundary (this is signaled in Fig. 8 by the abrupt reversal of the current predicted by the lower-band acceleration theorem), all three curves agree very well. Immediately afterwards, the calculated current follows fairly closely the dashed-dotted curve representing the prediction of the acceleration theorem for the undistorted chain. The dashed-dotted curve can be thought of as representing the limit of perfect Zener tunneling ($P=1$). In the present case, Zener breakdown is still not complete, however, since $P\simeq 0.93$. This means that when an electron approaches the Brillouin-zone boundary there is a small probability that instead of tunneling to the upper band, it will be Bragg reflected within the lower band and make a negative contribution to the current. This effect is clearly visible in Fig. 8, where each tunneling event is accompanied by an abrupt (but small) increase in the discrepancy between the calculated current and that predicted by the acceleration theorem for the undistorted chain. Notice also the rapidly damped high-frequency transient oscillations in the current which follow every tunneling event. It is clear that after a large number of such incomplete tunneling events between the lower and upper bands, the picture must become more complex since both bands will become appreciably populated by electrons of every allowed k state. As can be seen in Fig. 9, at later times the dominant frequency of the current is equal to that corresponding to the Zener period of the *undistorted* chain. (This is *twice* the period given by expression (43), which describes correctly the dominant period for the case of weak Zener tunneling shown in Fig. 7.) However, the current also has strong higher- and lower-frequency components.

The above examples show that the present two-band model is capable of describing Zener tunneling and that its predictions are quite reasonable physically, at least in simple cases which are readily accessible of semiquantitative analysis. It is also apparent that a multiplicity of other interesting tunneling regimes is yet to be explored.

D. Imperfect crystals

Until now we have considered crystals which, although dimerized, are perfectly periodic. Since Zener oscillations in metals are effectively damped out by scattering by impurities or other imperfections, it is interesting to consider the effect of deviations from perfect periodicity on the present class of systems. To this end we consider a perfectly dimerized chain with $u_n=(-1)^n u$ as above, but with one of the atoms being an "isoelectronic" impurity which is represented by adding a term $v_j c_j^\dagger c_j$ to the Hamiltonian (17) where j is the site of the impurity atom. The electron-density matrix at time $t=0$ is set up and its time evolution calculated as described in Sec. III A.

In Fig. 10 the response is shown of a dimerized 32-atom chain with one electron per atom without impurities (solid curve), and with two different isoelectronic impurities on site 1: $v_1=5$ eV (dashed curve) and $v_1=10$ eV (dashed-dotted curve). The system parameters u, t_0, α, and a, the limiting electric field $\tilde{E}$, and the rise time t_r are the same as for the 32-atom chain considered in Sec. III B

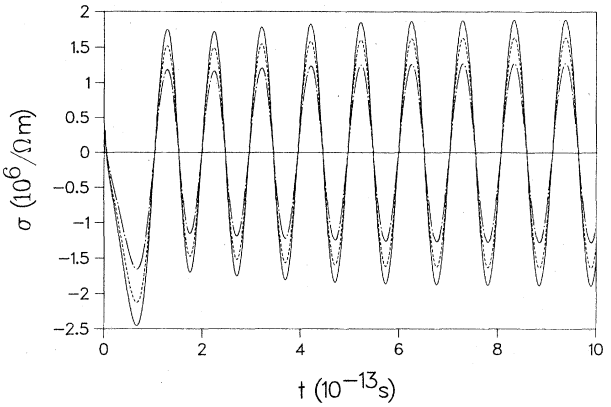

FIG. 10. Response of the same 32-atom chain as in Fig. 2 to the same electric field (solid curve); the same chain but with $v_1=5$ eV (dashed curve); the same chain but with $v_1=10$ eV (dashed-dotted curve).

so that we are in the insulator regime, far from Zener breakdown. In contrast to the case of Zener oscillations in a metal, the effect of the impurities on the current oscillations in the finite insulator is remarkably mild. The oscillations are still present, the period is the same, and there is no noticeable damping of the oscillations with time. Only the amplitude is reduced somewhat from the perfectly periodic case, by about 13% for the 5-eV impurity and 32% for the 10-eV impurity. The results for attractive impurities (negative v_j) were quite similar. Other static defects, which were produced by displacing a few atoms of the chain from their ideal positions given by $u_n=(-1)^n u$, were also studied and their effect on the current was similar to that of the isoelectronic impurities.

These results can be understood qualitatively if one regards the defects as perturbations which scatter electrons. Since in the finite insulator all of the one-electron states in the lower band are occupied, there are no empty states in the range of energies to which the electrons can be scattered by the imperfections. Thus, the influence of defects on the electron dynamics is minimal and the current oscillations which characterize electrical conduction in the finite insulator are very stable.

For comparision, the response of a 14-atom chain with one electron per atom and $u=0$ (a finite metal with a half-filled band) is shown in Fig. 11. The chosen parameters are $t_0=2.5$ eV, $a=1.22$ Å, $t_r=10^{-13}$ s, and $\tilde{E}=10^7$ V/m. The dashed-dotted curve is the response of this system in the absence of impurities, for times extending up to and slightly beyond one-quarter of the first Zener oscillation. Since $u=0$, we are not dealing here with a split band and the numerical calculation agrees with the prediction of the single-band acceleration theorem. The solid curve is the response of the same system but with an impurity located at atom 1 of the chain ($v_1=1$ eV). In this case the behavior is quite complex. Initially, the current follows very closely the results of the calculation for the system without impurities, but then a new regime is entered, characterized by abrupt near reversals of the current to negative values, each time followed by a relatively slow, oscillatory buildup of the current in the posi-

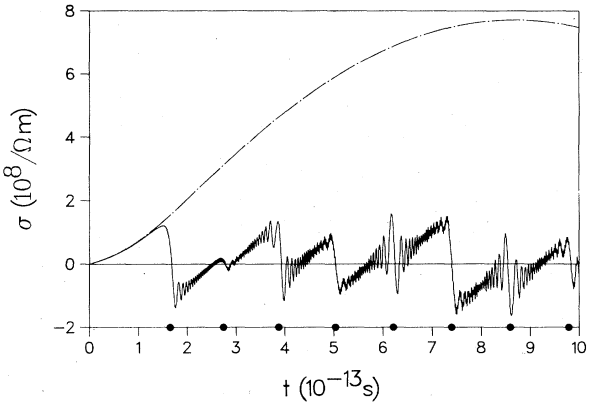

FIG. 11. Response of a metallic 14-atom chain with one electron per atom. $u=0$, $t_0=2.5$ eV, $a=1.22$ Å, $t_r=10^{-13}$ s, $\tilde{E}=10^7$ V/m. Dashed-dotted curve: perfect structure with no impurities. Solid curve: isoelectronic impurity on site 1; $v_1=1$ eV. Closed circles mark the times at which one-electron states at q come into resonance with those at $-q$.

tive direction. The details of each such cycle differ from those of the preceding one. One can understand physically what is happening as follows.

The impurity breaks the perfect periodicity of the system and can scatter electrons from one "unperturbed" single-particle state to another. However, this scattering is not very noticeable unless the two single-particle states are in resonance with each other. In practice, the resonance condition occurs when for two different one-electron states i and j, the q vectors, as defined in Eq. (15), obey $q_i=-q_j$. The times at which this condition is satisfied, as predicted by the single-band acceleration theorem, are indicated by the closed circles in Fig. 11. These times correlate very well with the abrupt reversals of the current. Thus, one can associate these current reversals with the scattering of an electron from q to $-q$ by the impurity when an occupied state at q comes into resonance with a nearly vacant one at $-q$. The high-frequency oscillations are then the signature of the transient associated with the scattering process. This interpretation is very close in spirit to the usual view of the role which elastic scattering plays in the Boltzmann equation describing electrical conduction in metals, and is consistent with the interpretation given above to the very different behavior of the oscillating currents in finite insulators.

IV. CONNECTION WITH THE LONDON THEORY OF RING CURRENTS

In the preceding sections we have considered conduction in linear chains of atoms with periodic boundary conditions in a uniform time-dependent vector potential. The problem of a closed ring of atoms in a magnetic field is a closely related one which has received much attention in the literature, although the emphasis has been on calculating magnetic susceptibilities and NMR chemical shifts which are due to the induced ring currents rather than the currents themselves. A comparison of the two approaches is clearly of interest.

The quantum theory for ring molecules in magnetic fields was first formulated by London[3] and developed further by a number of authors, notably by Pople[10] and McWeeny.[11] The basic formulation which has been used can be summarized briefly as follows.

The molecular orbitals in a static magnetic field are eigenfunctions of the Hamiltonian

$$H_A=(\mathbf{p}-q_e\mathbf{A})^2/2m+V(\mathbf{r}) , \tag{45}$$

where

$$\mathbf{B}=\nabla\times\mathbf{A} .$$

London chose basis functions of the form

$$\chi_s(\mathbf{r})=\phi_s(\mathbf{r})\exp(iq_e\mathbf{A}_s\cdot\mathbf{r}/\hbar) , \tag{46}$$

where ϕ_s is a modified tight-binding orbital of atom s and $\mathbf{A}_s$ is the vector potential at the center of atom s. Then the molecular orbitals are taken to be of the form

$$\Psi_j=\sum_s c_s\chi_s , \tag{47}$$

where the energy eigenvalues and coefficients c_s are determined using matrix elements of the Hamiltonian (45) in the basis (46). These matrix elements are given by

$$\begin{aligned}H_{st}&=\langle\chi_s\,|\,H_A\,|\,\chi_t\rangle\\&=\int d^3r\exp[-iq_e(\mathbf{A}_s-\mathbf{A}_t)\cdot\mathbf{r}/\hbar]\phi_s^*(\mathbf{r})\\&\quad\times\{[\mathbf{p}-q_e(\mathbf{A}-\mathbf{A}_t)]^2/2m+V(\mathbf{r})\}\phi_t(\mathbf{r}) .\end{aligned} \tag{48}$$

Taking the ϕ_t to be eigenstates of the intra-atomic part of the Hamiltonian in the curly brackets in (48) and approximating $\mathbf{r}$ in the exponent by

$$\mathbf{r}\cong\tfrac{1}{2}(\mathbf{R}_s+\mathbf{R}_t) , \tag{49}$$

where $\mathbf{R}_s+\mathbf{R}_t$ are the positions of atoms s and t, yields the London Hamiltonian

$$H_{st}=\beta_{st}\exp[-\tfrac{1}{2}iq_e(\mathbf{A}_s-\mathbf{A}_t)\cdot(\mathbf{R}_s+\mathbf{R}_t)\hbar] , \tag{50}$$

where

$$\beta_{st}=\int d^3r\,\phi_s^*(\mathbf{r})\{[p-q_e(\mathbf{A}-\mathbf{A}_t)]^2/2m+V(\mathbf{r})\}\phi_t(\mathbf{r}) . \tag{51}$$

For the purpose of calculating the effects of interatomic currents and for small fields, β_{st} is in practice usually approximated by its value for $A=0$, and only nearest-neighbor terms are considered. The eigenvalues of H_{st} and hence the magnetic susceptibility, which is due to circulating ring currents, and other quantities of interest are then calculated.

If a simple planar ring molecule is considered in a uniform magnetic field $\mathbf{B}$ perpendicular to the basal plane, then choosing $\mathbf{A}=-\frac{1}{2}\mathbf{r}\times\mathbf{B}$, the similarity between the London Hamiltonian (50) for the ring molecule and the forms (7) and (17) obtained in Sec. II for a linear chain in a uniform vector potential is striking. In fact, if we identify A in (7) and (17) with $|A_s|=|A_t|$ in (50), then it is easy to show that the Hamiltonians obtained in Sec. II are

the same as the London Hamiltonian (50) in the limit of large rings, except that the precise definitions of the matrix elements t and β are somewhat different. The similarity between the results obtained for the two different geometries can yield interesting insights into both situations.

While the London theory has been widely accepted as being substantially correct, it has also been criticized by some authors who have questioned the physical reality of the London ring currents.[12] Thus, an alternative derivation of the London Hamiltonian, such as has been given in Sec. II, is desirable, particularly since the simpler linear geometry which we have used avoids the need to make the somewhat crude approximation (49). Furthermore, the derivation in Sec. II shows clearly the importance of choosing a very special set of "tight-binding" basis functions ϕ_i for the theory, an aspect which appears to have received little recognition in the literature.

In comparing the work on ring currents with the present calculations, it should be noticed that the strength of the magnetic field in the case of magnetic susceptibility experiments corresponds roughly to the time variable in the results of Sec. III, although the magnetic fields used in practice correspond to extremely short times in the present work. Of course, the early transient behavior associated with the switching on of the field [for example, in Fig. 2(a)] is not reflected in the susceptibility measurements which are carried out in very slowly varying or steady magnetic fields. A positive current at short times (but after the decay of the initial transient) in the present calculations, corresponds to a diamagnetic susceptibility of the appropriate ring molecule; a negative current to a paramagnetic susceptibility. The annulenes (ring molecules of the type C_NH_N which are finite cyclic analogs of polyacetylene) are found experimentally to exhibit diamagnetic ring currents for $N=4n+2$ and paramagnetic ring currents for $N=4n$.[12(a)] This has previously been shown to be a direct consequence of the London theory,[10(b),12(a)] and is in agreement with the initial phases of the currents found in Sec. III for perfectly dimerized chains of the corresponding lengths (Figs. 4 and 2, respectively).

ACKNOWLEDGMENTS

I would like to thank R. Barrie, D. Murray, M. Plischke, J. Thewalt, and S. E. Ulloa for useful discussions and comments, and F. Kirczenow for helping me to read London's paper. This work was supported by the Natural Sciences and Engineering Research Council of Canada.

---

[1]The atoms are assumed to be static and their positions to be adjustable to specification. The case in which the atoms are allowed to move will be considered in a subsequent paper.

[2]C. L. Roy and P. K. Mahapatra, J. Phys. C **17**, 437 (1984).

[3]F. London, J. Phys. Radium **8**, 397 (1937).

[4]A critique of some derivations of (16) has been given by J. Zak, in *Solid State Physics,* edited by H. Ehrenreich, F. Seitz, and D. Turnbull (Academic, New York, 1972), Vol. 27.

[5]C. L. Roy and P. K. Mahaptra, J. Phys. C **13**, 5365 (1980); P. Roblin and M. W. Muller, *ibid.* **16**, 4547 (1983).

[6]The application of (16) to the closely related problem of circulating currents in small one-dimensional rings of normal metal driven by a time-dependent magnetic flux has recently been discussed by M. Büttiker, Y. Imry, and R. Landauer, Phys. Lett. **96A**, 365 (1983); and R. Landauer and M. Büttiker, Phys Rev. Lett. **54**, 2049 (1985), without reference to tight-binding models.

[7]See, W. P. Su, J. R. Schrieffer, and A. J. Heeger, Phys. Rev. B **22**, 2099 (1980); **28**, 1138(E) (1983), for a detailed discussion.

[8]R. E. Peierls, *Quantum Theory of Solids* (Oxford University Press, London, 1964), p. 108.

[9]See, J. M. Ziman, *Principles of the Theory of Solids* (Cambridge University Press, Cambridge, England, 1972), pp. 190—196.

[10]J. A. Pople, Mol. Phys. **1**, 175 (1958); J. A. Pople and K. G. Untch, J. Am. Chem. Soc. **88**, 4811 (1966).

[11]R. McWeeny, Mol. Phys. **1**, 311 (1958).

[12]See, A. J. Jones, Rev. Pure Appl. Chem. **18**, 253 (1968), for a review; and Y. B. Vysotsky, V. A. Kuzmitsky, and K. N. Solovyov, Theor. Chim. Acta **59**, 467 (1981), for a more recent brief survey of the literature.